Inorganic Chemistry
Article

Inorg. Chem. **2010**, *49*, 8351–8357 **8351**
DOI: 10.1021/ic1009658

New Efficient Ruthenium Sensitizers with Unsymmetrical Indeno[1,2-*b*]thiophene or a Fused Dithiophene Ligand for Dye-Sensitized Solar Cells

Jeum-Jong Kim,[†] Kimin Lim,[†] Hyunbong Choi,[†] Shengqiang Fan,[†] Moon-Sung Kang,[‡] Guohua Gao,[§] Hong Seok Kang,[∥] and Jaejung Ko*[,†]

[†]*Department of Material Chemistry, Korea University, Jochiwon, Chungnam 339-700, Korea,*
[‡]*Energy Laboratory, Samsung SDI Corporate R&D Center, Yongin-si, Gyenggi-do 449-577, Korea,*
[§]*Pohl Institute of Solid State Physics, Tongji University, Shanghai 200092, People's Republic of China, and*
[∥]*Department of Nano and Advanced Materials, College of Engineering, Jeonju University, Hyoja-dong, Wansan-ku, Chonju, Chonbuk 560-759, Republic of Korea*

Received May 14, 2010

Two novel ruthenium sensitizers containing unsymmetrical indeno[1,2-*b*]thiophene or a fused dithiophene unit in the ancillary ligand have been designed and synthesized. The photovoltaic performance of **JK-188** using an electrolyte consisting of 0.6 M 1,2-dimethyl-3-propylimidazolium iodide, 0.05 M I_2, 0.1 M LiI, 0.05 M guanidinium thiocyanate, and 0.5 M *tert*-butylpyridine in acetonitrile revealed a short-circuit photocurrent density of 18.60 mA/cm^2, an open-circuit voltage of 0.72 V, and a fill factor of 0.71, yielding an overall conversion efficiency of 9.54%. The cell exhibits a remarkable stability under 1000 h of light soaking at 60 °C using a quasi-solid-state electrolyte consisting of 5 wt % poly(vinylidenefluoride-*co*-hexafluoropropylene), 0.6 M 1-propyl-2,3-dimethylimidazolium iodide, 0.5 M *N*-methylbenzimidazole, and 0.1 M I_2 in 3-methoxypropionitrile, retaining 97% of the initial efficiency (7.38%).

Introduction

The development of cost-effective renewable energy alternatives to current power generation methods is in urgent need because of the increasing energy demands and concerns over global warming. Among several new energy technologies, dye-sensitized solar cells (DSSCs) have attracted significant attention because of their low cost and high performance.[1] These cells employ mostly polypyridylruthenium complexes as charge-transfer sensitizers. Until now, only four polypyridylruthenium sensitizers have achieved power conversion efficiencies over 11%.[2] *cis*-Bis(thiocyanato)bis(2,2′-bipyridyl-4,4′-dicarboxylato)ruthenium bis(tetrabutylammonium) (**N719**) has maintained a clear lead because of its outstanding performance. In spite of high photovoltaic performances, the efficiency of DSSCs needs to be improved in order to become competitive with conventional photovoltaic cells. One of the possible approaches to address this issue is to increase a spectral response of the sensitizer in the low energies. Such an enhancement of the light-harvesting ability and a red shift of the metal-to-ligand charge-transfer (MLCT) band can be achieved by extending the π conjugation of the ancillary ligand[3] or modifying the ancillary ligand with electron-donating units.[4] A successful strategy for enhancing the device efficiency consists of the replacement of one of the 4,4′-dicarboxy-2,2′-bipyridine (dcbpy) anchoring ligands in $[Ru(dcbpyH_2)_2(NCS)_2]$ (**N3**) with a conjugated ancillary group.[5]

Wu et al.[6] and other groups[7] have developed very efficient ruthenium sensitizers with an extended π-conjugated ancillary

*To whom correspondence should be addressed. E-mail: jko@korea.ac.kr. Tel: 82 41 860 1337. Fax: 82 41 867 5396.

(1) (a) O'Regan, B.; Grätzel, M. *Nature* **1991**, *353*, 737. (b) Grätzel, M. *Nature* **2001**, *414*, 338.

(2) (a) Nazeeruddin, M. K.; De Angelis, F.; Fantacci, S.; Selloni, A.; Viscardi, G.; Liska, P.; Ito, S.; Takeru, B.; Grätzel, M. *J. Am. Chem. Soc.* **2005**, *127*, 16835. (b) Chiba, Y.; Islam, A.; Watanabe, Y.; Komiya, R.; Koide, N.; Han, L. *Jpn. J. Appl. Phys.* **2006**, *45* (Part 2), L638. (c) Gao, F.; Wang, Y.; Shi, D.; Zhang, J.; Wang, M.; Jing, X.; Humphry-Baker, R.; Wang, P.; Zakeeruddin, S. M.; Grätzel, M. *J. Am. Chem. Soc.* **2008**, *130*, 10720. (d) Cao, Y.; Bai, Y.; Yu, Q.; Cheng, Y.; Liu, S.; Shi, D.; Gao, F.; Wang, P. *J. Phys. Chem. C* **2009**, *113*, 6290.

(3) (a) Jang, S.-R.; Lee, C.; Choi, H.; Ko, J.; Lee, J.; Vittal, R.; Kim, K.-J. *Chem. Mater.* **2006**, *18*, 5604. (b) Kim, C.; Choi, H.; Kim, S.; Baik, C.; Song, K.; Kang, M.-S.; Kang, S. O.; Ko, J.; Humphry-Baker, R.; Grätzel, M.; Nazeeruddin, M. K. *Inorg. Chem.* **2008**, *47*, 2267.

(4) (a) Karthikeyan, C.; Wietasch, H.; Thelakkat, M. *Adv. Mater.* **2007**, *19*, 1091. (b) Chen, C.-Y.; Chen, J.-G.; Wu, S.-J.; Li, J.-Y.; Wu, C.-G.; Ho, K.-C. *Angew. Chem., Int. Ed.* **2008**, *47*, 7432. (c) O'Regan, B. C.; Walley, K.; Juozapavicius, M.; Anderson, A.; Mater, F.; Ghaddar, T.; Zakeeruddin, S. M.; Klein, C.; Durrant, J. R. *J. Am. Chem. Soc.* **2009**, *131*, 3541. (d) Abbotto, A.; Barolo, C.; Bellotto, L.; De Angelis, F.; Grätzel, M.; Manfredi, N.; Marinzi, C.; Fantacci, S.; Yum, J.-H.; Nazeeruddin, M. K. *Chem. Commun.* **2008**, 5318.

(5) Nazeeruddin, M. K.; Kay, A.; Rodicio, I.; Humphry-Baker, R.; Muller, E.; Liska, P.; Vlachopoulos, N.; Grätzel, M. *J. Am. Chem. Soc.* **1993**, *115*, 6382.

(6) (a) Chen, C.-Y.; Wu, S.-J.; Wu, C.-G.; Ho, K.-C.; Chen, J.-G.; Ho, K.-C. *Angew. Chem., Int. Ed.* **2006**, *45*, 5882. (b) Chen, C.-Y.; Wu, S.-J.; Li, J.-Y.; Wu, C.-G.; Chen, J.-G.; Ho, K.-C. *Adv. Mater.* **2007**, *19*, 3888. (c) Chen, C.-Y.; Lu, H.-C.; Wu, C.-G.; Chen, J.-G.; Ho, K.-C. *Adv. Funct. Mater.* **2007**, *17*, 29.

Published on Web 08/26/2010

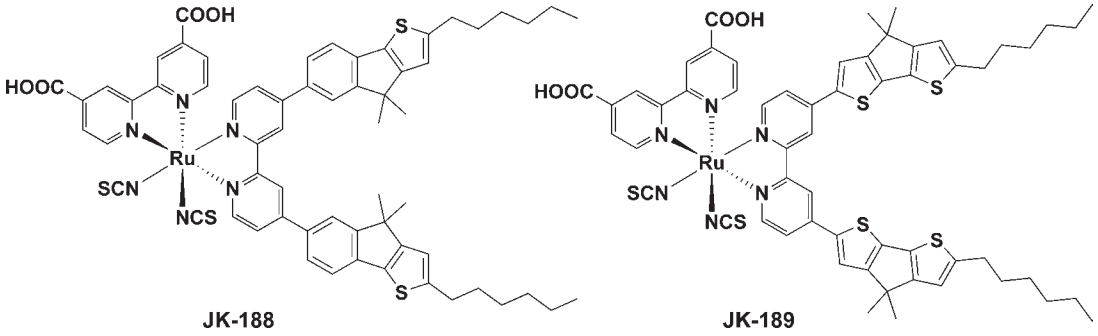

Figure 1. Molecular structures of **JK-188** and **JK-189**.

group such as thiophene derivatives and alkoxybenzene moieties. However, in spite of the many advantages shown by these ruthenium sensitizers, few of them have surpassed **N719** for use in terms of its cost and efficiency.[2c] Thus, the systematic design of efficient ruthenium sensitizers, comparable to or better than **N719**, is strongly required. It is well established that a phenyl[8] or thiophene[9] group substituted to an ancillary polypyridyl ligand in ruthenium sensitizers causes a red shift and increases an absorption coefficient of the MLCT band. Because even small structural modifications of sensitizers result in significant changes in redox energies and threshold wavelengths, the two ruthenium sensitizers, **JK-188** and **JK-189**, are molecularly engineered in such a way as to have a red shift and a high absorption coefficient of the MLCT band with respect to **N719** through a combination of phenyl, thiophenyl, and hexyl groups, with its photovoltaic performance being better than **N719** under the same fabrication conditions. Here we report the synthesis of amphiphilic ruthenium sensitizers containing indeno[1,2-*b*]-thiophene or cyclopenta[2,1-*b*:3,4-*b*′]dithiophene units and their excellent photovoltaic performances in DSSCs. The molecular structures of the two ruthenium sensitizers are shown in Figure 1.

Experimental Section

All reagents were obtained from commercial sources and were used as received. Solvents were dried over sodium, CaH_2, or P_2O_5 and distilled before use.

All of the reactions were carried out under a nitrogen atmosphere. ^1H and ^{13}C NMR spectra were recorded on a Varian Mercury 300 spectrometer. UV/vis spectra were recorded using a 1-cm-path-length quartz cell on a Cary 5 spectrophotometer.

Photoelectrochemical data were measured using a 1000 W xenon light source (Oriel 91193) that was focused to give 1000 W/m^2, the equivalent of one sun at air mass (AM) 1.5, at the surface of the test cell. The light intensity was adjusted with a silicon solar cell that was double-checked with an NREL-calibrated silicon solar cell (PV Measurement Inc.). The applied potential and measured cell current were measured using a Keithley model 2400 digital source meter. The current−voltage characteristics of the cell under these conditions were determined by biasing the cell externally and measuring the generated photocurrent. This process was fully automated using *Wavemetrics* software.

Fluorine-doped tin oxide (FTO) glass plates (Pilkington TEC Glass-TEC 8; solar 2.3 mm thickness) were cleaned in a detergent solution using an ultrasonic bath for 30 min and then rinsed with water (H_2O) and ethanol (EtOH). Then, the plates were immersed in 40 mM $TiCl_4$(aq) at 70 °C for 30 min and washed with H_2O and EtOH. A transparent nanocrystalline layer was prepared on the FTO glass plates by using a doctor blade printing TiO_2 paste (Solaronix, Ti-Nanoxide T/SP), which was then dried for 2 h at 25 °C. The TiO_2 electrodes were gradually heated under an air flow at 325 °C for 5 min, at 375 °C for 5 min, at 450 °C for 15 min, and at 500 °C for 15 min. The thickness of the transparent layer was measured using an Alpha-step 250 surface profilometer (Tencor Instruments, San Jose, CA). A paste containing 400-nm-sized anatase particles (CCIC PST-400C) was deposited by means of doctor blade printing to obtain the scattering layer and then dried for 2 h at 25 °C. The TiO_2 electrodes were gradually heated under an air flow at 500 °C for 30 min. The resulting film was composed of a 10-μm-thick transparent layer and a 4-μm-thick scattering layer. The TiO_2 electrodes were treated again with $TiCl_4$ at 70 °C for 30 min and sintered at 500 °C for 30 min. Then, they were immersed in **JK-188** (0.3 mM in CH_3CN/*t*-BuOH) and **JK-189** (0.3 mM in EtOH) solutions and kept at room temperature for 24 h. FTO plates for the counter electrodes were cleaned in an ultrasonic bath in H_2O, acetone, and 0.1 M aqueous HCl, subsequently. The counter electrodes were prepared by placing a drop of an H_2PtCl_6 solution (2 mg of Pt in 1 mL of EtOH) on an FTO plate and heating (at 400 °C) for 15 min. The dye-adsorbed TiO_2 electrodes and the platinum counter electrodes were assembled into a sealed sandwich-type cell by heating at 80 °C using a hot-melt ionomer film (Surlyn) as a spacer between the electrodes. A drop of the electrolyte solution was placed in the drilled hole of the counter electrode and was driven into the cell via vacuum backfilling. Finally, the hole was sealed using additional Surlyn and a cover glass (0.1 mm thickness).

The electron diffusion coefficients (D_e) and lifetimes (τ_e) in TiO_2 photoelectrodes were measured by the stepped light-induced transient measurements of photocurrent and voltages.[18−21] The transients were induced by a stepwise change in the laser intensity. A diode laser (λ = 635 nm) as a light source was modulated using a function generator. The

(7) (a) Wang, P.; Zakeeruddin, S. M.; Moser, J.-E.; Humphry-Baker, R.; Comte, P.; Aranyos, V.; Hagfeldt, A.; Nazeeruddin, M. K.; Grätzel, M. *Adv. Mater*. **2004**, *16*, 1806. (b) Wang, P.; Klein, C.; Humphry-Baker, R.; Zakeeruddin, S. M.; Grätzel, M. *J. Am. Chem. Soc*. **2005**, *127*, 808. (c) Kuang, D.; Klein, C.; Ito, S.; Moser, J.-E.; Humphry-Baker, R.; Evans, N.; Duriaux, F.; Grätzel, C.; Zakeeruddin, S. M.; Grätzel, M. *Adv. Mater*. **2007**, *19*, 1133. (d) Gao, F.; Wang, Y.; Zhang, J.; Shi, D.; Wang, M.; Humphry-Baker, R.; Wang, P.; Zakeeruddin, S. M.; Grätzel, M. *Chem. Commun*. **2008**, 2635.

(8) (a) Phifer, C. C.; McMillin, D. R. *Inorg. Chem*. **1986**, *25*, 1329. (b) Kalyanasundaram, K.; Nazeeruddin, M. K.; Grätzel, M.; Viscardi, G.; Savarino, P.; Barni, E. *Inorg. Chem. Acta* **1992**, *198−200*, 831. (c) Constable, E. C.; Cargill Thompson, A. M. W.; Tocher, D. A.; Daniels, M. A. M. *New J. Chem*. **1992**, *16*, 855. (d) Maestri, M.; Armaroli, N.; Balzani, V.; Constable, E. C.; Cargill Thompson, A. M. W. *Inorg. Chem*. **1995**, *34*, 2759.

(9) (a) Jiang, K.-J.; Masaki, N.; Xia, J.; Noda, S.; Yanagida, S. *Chem. Commun*. **2006**, 2460. (b) Shi, D.; Pootrakulchote, N.; Li, R.; Gui, J.; Wang, Y.; Zakeeruddin, S. M.; Grätzel, M.; Wang, P. *J. Phys. Chem. C* **2008**, *112*, 17046. (c) Gao, F.; Wang, Y.; Shi, D.; Zhang, J.; Wang, M.; Jing, X.; Humphry-Baker, R.; Wang, P.; Zakeeruddin, S. M.; Grätzel, M. *J. Am. Chem. Soc*. **2008**, *130*, 10720.

Scheme 1. Schematic Diagram for the Synthesis of Ruthenium Sensitizers **JK-188** and **JK-189**[a]

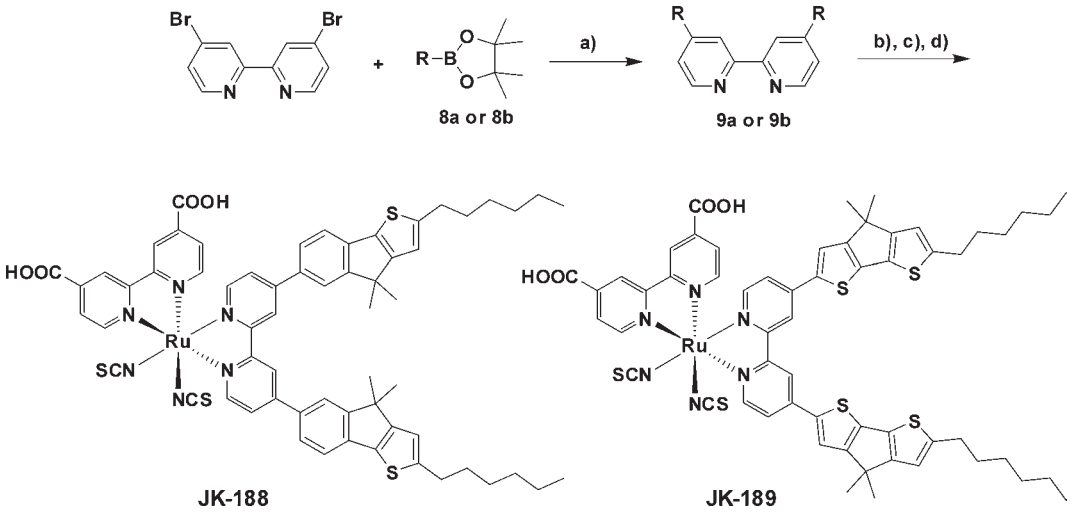

[a] Reagents: (a) **8a** or 2-(6-hexyl-4,4′-dimethylcyclopenta[2,1-*b*:3,4-*b*′]dithiophenyl-4,4,5,5-tetramethyl-1,3,2-dioxaborolane (**8b**), $Pd(PPh_3)_4/Na_2CO_3$, THF/H_2O. (b) $[Ru(Cl)_2(p\text{-cymene})]_2$, DMF, 70 °C. (c) Bis(2,2′-bipyridyl)-4,4′-dicarboxylic acid, DMF, reflux. (d) NH_4NCS, DMF, 140 °C.

initial laser intensity was a constant 90 mW/cm^2 and was attenuated to approximately 10 mW/cm^2 using an ND filter, which was positioned at the front side of the fabricated samples (TiO_2 film thickness = ca. 8 μm; active area = 0.04 cm^2). The photocurrent and photovoltage transients were monitored using a digital oscilloscope through an amplifier. The D_e value was obtain by a time constant (τ_e) determined by the fitting of a decay of the photocurrent transient with $\exp(-t/\tau_e)$ and the TiO_2 film thickness (ω) using the equation $D_e = \omega^2/(2.77\tau_e)$.[18] The τ_e value was also determined by the fitting of a decay of the photovoltage transient with $\exp(-t/\tau_e)$.[18] All experiments were carried out at room temperature.

4,4′-Bis(2-hexyl-4,4-dimethyl-4*H*-indeno[1,2-*b*]thiophen-6-yl)-bipyridine (9a). 2-(2-Hexyl-4,4-dimethyl-4*H*-indeno[1,2-*b*]thiophen-6-yl)-4,4,5,5-tetramethyl-1,3,2-dioxaborolane (**8a**; 3 mmol), 4,4′-dibromo-2,2′-bipyridyl (1 mmol), $Pd(PPh_3)_4$ (5 mol %), and K_2CO_3 (15 mmol) were dissolved in tetrahydrofuran (THF; 50 mL)/H_2O (10 mL), and the mixture was refluxed for 15 h. After evaporation of the solvent under reduced pressure, H_2O (10 mL) and dichloromethane (40 mL) were added. The organic layer was separated and dried in $MgSO_4$. The solvent was removed under reduced pressure. The pure product **9a** was obtained by column chromatography on silica gel (ethyl acetate, R_f = 0.41). ^{1}H NMR ($CDCl_3$): δ 8.77 (s, 2H), 7.76 (d, 2H, J = 2.7 Hz), 7.77 (s, 2H), 7.70 (d, 2H, J = 7.8 Hz), 7.62 (dd, 2H, J = 5.1 Hz), 7.45 (d, 2H, J = 7.8 Hz), 6.78 (s, 2H), 2.88 (t, 4H, J = 7.8 Hz), 1.74 (m, 4H), 1.52 (s, 12H), 1.44−1.33 (m, 12H), 0.91 (t, 6H, J = 6.9 Hz). ^{13}C NMR ($CDCl_3$): δ 159.4, 156.9, 156.5, 150.8, 149.9, 149.7, 138.4, 136.3, 134.5, 126.4, 121.6, 121.0, 119.1, 119.8, 118.1, 46.1, 31.9, 31.7, 31.4, 29.0, 26.1, 22.7, 14.2. Anal. Calcd for $C_{48}H_{52}N_2S_2$: C, 79.95; H, 7.27; N, 3.88. Found: C, 79.76; H, 7.22; N, 3.72.

4,4′-Bis(6-hexyl-4,4′-dimethylcyclopenta[2,1-*b*:3,4-*b*′]dithiophen-2-yl)-2,2′-bipyridine (9b). 2-(6-Hexyl-4,4′-dimethylcyclopenta-[2,1-*b*:3,4-*b*′]dithiophen-2-yl-4,4,5,5-tetramethyl-1,3,2-dioxaborolane (**8b**; 3.6 mmol), 4,4′-dibromo-2,2′-bipyridyl (1.2 mmol), $Pd(PPh_3)_4$ (5 mol %), and K_2CO_3 (6 mmol) were dissolved in THF (30 mL)/H_2O (6 mL), and the mixture was refluxed for 15 h. After evaporation of the solvent under reduced pressure, H_2O (20 mL) and dichloromethane (50 mL) were added. The organic layer was separated and dried in $MgSO_4$. The solvent was removed under reduced pressure. The pure product was obtained by column chromatography on silica gel (ethyl acetate, R_f = 0.35). ^{1}H NMR ($CDCl_3$): δ 0.88 (m, 6H), 1.32 (m, 12H), 1.48 (s, 12H), 1.70 (m, 4H), 2.83 (m, 4H), 6.73 (s, 2H), 7.45 (d, 2H, J = 7.8 Hz), 7.62 (d, 2H, J = 7.8 Hz), 8.63 (m, 4H). ^{13}C NMR ($CDCl_3$): δ 161.2, 160.2, 156.2, 149.6, 148.9, 143.5, 139.8, 132.1, 127.4, 119.8, 118.9, 118.3, 116.2, 45.7, 32.0, 31.8, 31.3, 29.1, 25.3, 22.8, 14.4. Anal. Calcd for $C_{44}H_{48}N_2S_4$: C, 72.08; H, 6.60; N, 3.82. Found: C, 71.86; H, 6.48; N, 3.68.

***cis*-Bis(thiocyanato)(2,2′-bipyridyl-4,4′-dicarboxylato){4-bis-(2-hexyl-4,4-dimethyl-4*H*-indeno[1,2-*b*]thiophen-6-yl)bipyridyl}-ruthenium(II) (JK-188).** A mixture of **9a** (0.41 mmol) and a dichloro(*p*-cymene)ruthenium(II) dimer (0.2 mmol) in argon-degassed *N*,*N*-dimethylformamide (DMF; 15 mL) was stirred at 70 °C for 4 h under reduced light. Subsequently, 4,4′-dicarboxyl-2,2′-bipyridine (0.41 mmol) was added into the flask, and the reaction mixture was refluxed for 4 h. Then, an excess of NH_4NCS (4.1 mmol) was added to the resulting dark solution, and the reaction continued for another 4 h at 140 °C. The reaction mixture was cooled down to room temperature, and the solvent was removed under vacuum. H_2O was added to induce the precipitate. The resulting solid was filtered and washed with H_2O and dried under vacuum. The resulting solid was dissolved in methanol (MeOH) containing 2.5 equiv of tetrabutylammonium hydroxide to confer solubility by deprotonation of the carboxylic group and purified on a Sephadex LH-20 column with MeOH as the eluent. The collected main band was concentrated, and the solution pH was lowered to 5.1 using 0.02 M nitric acid. The precipitate was collected on a sintered glass crucible by suction filtration and dried in air. Yield: 50%. IR (KBr, cm^{-1}): 3070, 2957, 2925, 2870, 2102, 1726, 1601, 1538, 1458, 1434, 1362, 1231, 1020. ^{1}H NMR (CD_3OD): δ 9.57 (d, 1H, J = 5.1 Hz), 9.28 (d, 1H, J = 5.1 Hz), 8.96 (s, 1H), 8.79 (s, 1H), 8.64 (s, 1H), 8.51 (s, 1H), 8.20 (d, 1H, J = 4.8 Hz), 7.91 (s, 1H), 7.81 (d, 1H, J = 7.2 Hz), 7.70−7.46 (m, 7H), 7.26 (d, 1H, J = 5.4 Hz), 7.07 (s, 1H), 6.80 (d, 2H, J = 11.4 Hz), 2.81 (t, 4H, J = 6.0 Hz), 1.57−1.30 (m, 28H), 0.95−0.84 (m, 6H). Anal. Calcd for $C_{62}H_{60}N_6O_4RuS_4$: C, 62.97; H, 5.11; N, 7.11. Found: C, 62.78; H, 5.01; N, 6.84.

***cis*-Bis(thiocyanato)(2,2′-bipyridyl-4,4′-dicarboxylato){4,4′-bis-(6-hexyl-4,4′-dimethylcyclopenta[2,1-*b*:3,4-*b*′]dithiophen-2-yl)-2,2′-bipyridyl}ruthenium(II) (JK-189).** The product was prepared using the same procedure of **JK-188** except that **9b** was used instead of **9a**. Yield: 52%. IR (KBr, cm^{-1}): 3038, 2957, 2924, 2854, 2100, 1731, 1610, 1536, 1449, 1425, 1386, 1231, 1018. ^{1}H NMR (CD_3OD): δ 9.58 (d, 1H, J = 5.1 Hz), 9.07 (d, 1H, J = 5.1 Hz), 8.93 (s, 1H), 8.76 (s, 1H), 8.44 (s, 1H), 8.38 (s, 1H), 8.29 (s, 1H), 8.15 (m, 3H), 7.56 (m, 2H), 7.49 (s, 1H), 7.26 (d, 1H, J = 5.4 Hz), 6.93 (s, 1H), 6.87 (s, 1H), 2.95−2.85 (m, 4H), 1.76−1.66 (m, 4H), 1.37 (s, 12H), 1.30 (m, 12H), 0.92 (m, 6H). Anal. Calcd

for $C_{56}H_{52}N_6O_4RuS_4$: C, 61.01; H, 4.75; N, 7.04. Found: C, 60.86; H, 4.62; N, 6.68.

Results and Discussion

The two ruthenium sensitizers **JK-188** and **JK-189** have been synthesized by the stepwise synthetic protocol illustrated in Scheme 1. There are two key starting compounds, **8a** and **8b**, for the synthesis of two ruthenium sensitizers. The synthesis of **8a** was prepared in five steps starting from methyl-5-bromo-2-(5-hexylthiophene-2-yl)benzoate. The second compound **8b** was synthesized in four steps beginning with 4*H*-cyclopenta-[2,1-*b*:3,4-*b*′]dithiophene (see the Supporting Information). The Suzuki coupling reaction[10] of 4,4′-dibromobipyridine with **8a** and **8b** gave **9a** and **9b**. **JK-188** and **JK-189** were synthesized in a one-pot reaction from the sequential reaction of [Ru(*p*-cymene)Cl_2]$_2$ with **9a** and **9b**, followed by the reaction of the resulting ruthenium complex with 4,4′-dicarboxyl-2,2′-bipyridine. The dichlororuthenium complexes reacted with an excess of ammonium thiocyanate to afford the ruthenium sensitizers **JK-188** and **JK-189**. The sensitizers **JK-188** and **JK-189** were spectroscopically characterized, and all data are consistent with the formulated structures.

The UV/vis and emission spectra of **JK-188** and **JK-189** in EtOH are shown in Figure 2a, together with the **N719** absorption spectrum as a reference. The strong absorption band of **JK-188** and **JK-189** around 310 nm is due to a bipyridine intraligand $\pi-\pi^*$ transition. The absorption spectra of both sensitizers in the visible region are dominated by MLCT transitions. The low-energy MLCT absorption band of **JK-189** at 543 nm is about 21 and 23 nm red-shifted compared to that of **JK-188** and **N719**, respectively. The measured molar extinction coefficient (ε) at 543 nm for **JK-189** is 15 865 M^{-1} cm^{-1}, which is higher than the corresponding values for **JK-188** (15 640 M^{-1} cm^{-1}) and **N719** (14 400 M^{-1} cm^{-1}). The higher light harvesting of **JK-189** compared with that of **JK-188** and **N719** is attributable to an electron-donating ability in an ancillary ligand and an increased highest occupied molecualr orbital (HOMO) energy level. The absorption spectra of **JK-188** and **JK-189** on a TiO_2 film are red-shifted and broaden because of the *J* aggregation and interaction of the anchoring group with the surface titanium ion, ensuring a good light-harvesting efficiency (Figure 2b). Excitation of the low-energy MLCT band of **JK-188** and **JK-189** resulted in a strong emission centered at 721 and 778 nm, respectively.

To evaluate the feasibility of electron transfer from the excited state of the sensitizers to the conduction band of the TiO_2 electrode, we carried out cyclic voltammetry experiments on **JK-188** and **JK-189** in CH_3CN with $TBAPF_6$ as the supporting electrolyte. Both **JK-188** and **JK-189** adsorbed on TiO_2 films show a single quasi-reversible oxidation at 0.98 and 0.93 V versus NHE, respectively, which is assigned to the $Ru^{II/III}$ redox couple. The values may be compared to 1.12 V versus NHE measured for **N3**. The 0.19 V cathodic shift of the **JK-189** oxidation potential compared to that of **N3** is attributable to the influence of the electron-rich dithiophene

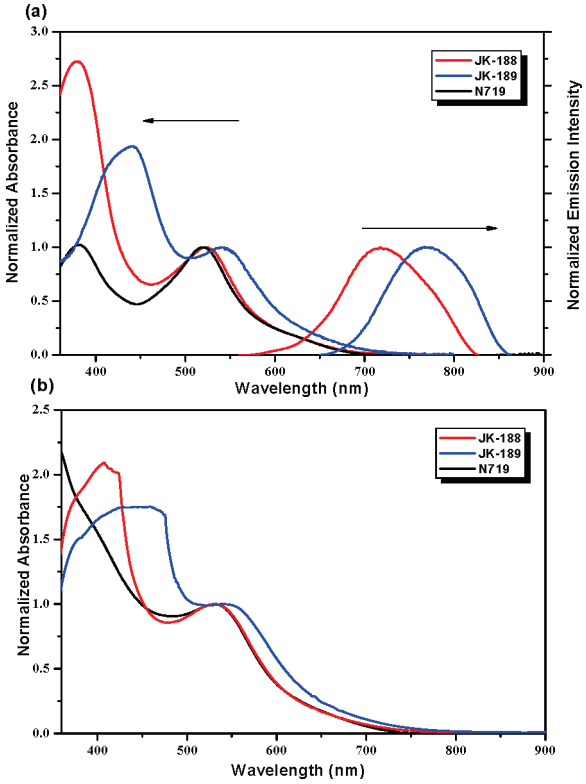

Figure 2. Absorption and emission spectra (a) of **JK-188** (red line), **JK-189** (blue line), and **N719** (black line) in EtOH and absorption spectra (b) of **JK-188** (red line), **JK-189** (blue line), and **N719** (black line) adsorbed on a TiO_2 film.

donor rings. The oxidation potential of both sensitizers is energetically favorable for iodide oxidation.[5] The excited-state reduction potential of **JK-188** and **JK-189** calculated from the oxidation potential and E_{0-0}[11] are listed in Table 1. The excited-state oxidation potentials (E^*_{ox}) of the sensitizers (**JK-188**, −0.97 V vs NHE; **JK-189**, −0.90 V vs NHE) are much more negative than the conduction band level of TiO_2 at approximately −0.5 V versus NHE, ensuring the thermodynamic driving force for charge injection.[12]

In order to evaluate the photophysical properties, molecular orbital calculations on **JK-188** and **JK-189** were performed with the local density approximation within the projected augmented wave.[13] Figure 3 presents the isodensity plots of the frontier molecular orbitals of **JK-188** and **JK-189**. The calculation illustrates that the HOMO and HOMO−1 of both sensitizers exhibit ruthenium t_{2g} character and a sizable population from the thiocyanate with a significant contribution on the far-end sulfur atom. The lowest unoccupied molecualr orbital (LUMO) of both sensitizers are predominately delocalized over the dcbpy ligand and ruthenium center. In the case of the LUMO+1 of **JK-189**, the LUMO+1 is a combination of the π-bonding orbital of the dcbpy and the ruthenium center, appreciably mixed with the bpy of the ancillary ligand. Because light excitation is associated with the vectorial electron flow from the HOMO to the LUMO,

(10) (a) Hoffmann, K. J.; Bakken, E.; Samuelsen, E. J.; Carlsen, P. H. *J. Synth. Met.* **2000**, *113*, 39. (b) Huang, C.-H.; McClenaghan, N. D.; Kuhn, A.; Hofstraat, J. W.; Bassan, D. M. *Org. Lett.* **2005**, *7*, 3409. (c) Turbiez, M.; Frére, P.; Allain, M.; Videlot, C.; Ackermann, J.; Roncali, J. *Chem.—Eur. J.* **2005**, *11*, 3742.

(11) Li, X.; Hou, X.; Duan, F.; Huang, C. *Inorg. Chem. Commun.* **2006**, *9*, 394.

(12) (a) Bond, A. M.; Deacon, G. B.; Howitt, J.; MacFarlane, D. R.; Spiccia, L.; Wolfbauer, G. *J. Electrochem. Soc.* **1999**, *146*, 648. (b) Wang., P.; Zakeeruddin, S. M.; Moser, J.-E.; Grätzel, M. *J. Phys. Chem. B* **2003**, *107*, 13280.

(13) Kresse, G.; Joubert, D. *Phys. Rev. B* **1999**, *59*, 1758.

Table 1. Optical, Oxidation, and DSSC Performance Parameters of Dyes

dye	λ_{abs}[a]/nm (ε/M^{-1} cm^{-1})	E_{ox}[b]/V	E_{0-0}[c]/V	E_{LUMO}[d]/V	J_{sc}/(mA/cm^2)	V_{oc}/V	FF	η[e]/%
JK-188	522 (15 640), 378 (42 600)	0.98	1.95	−0.97	18.60	0.72	0.71	9.54
JK-189	543 (15 865), 440 (30 762)	0.93	1.83	−0.90	18.90	0.63	0.73	8.70
N719	520 (14 400), 380 (14 682)				16.28	0.76	0.73	9.00

[a] Absorption spectra were measured in an EtOH solution. [b] Oxidation potentials of dyes on TiO_2 were measured in CH_3CN with 0.1 M (n-$C_4H_9)_4NPF_6$ with a scan rate of 50 mV/s (vs NHE). [c] E_{0-0} was determined from the intersection of absorption and emission spectra in EtOH. [d] E_{LUMO} was calculated by $E_{ox} - E_{0-0}$. [e] Performances of DSSCs were measured with a 0.18 cm^2 working area. Electrolyte: 0.6 M DMPII, 0.05 M I_2, 0.1 M LiI, and *tert*-butylpyridine in acetonitrile.

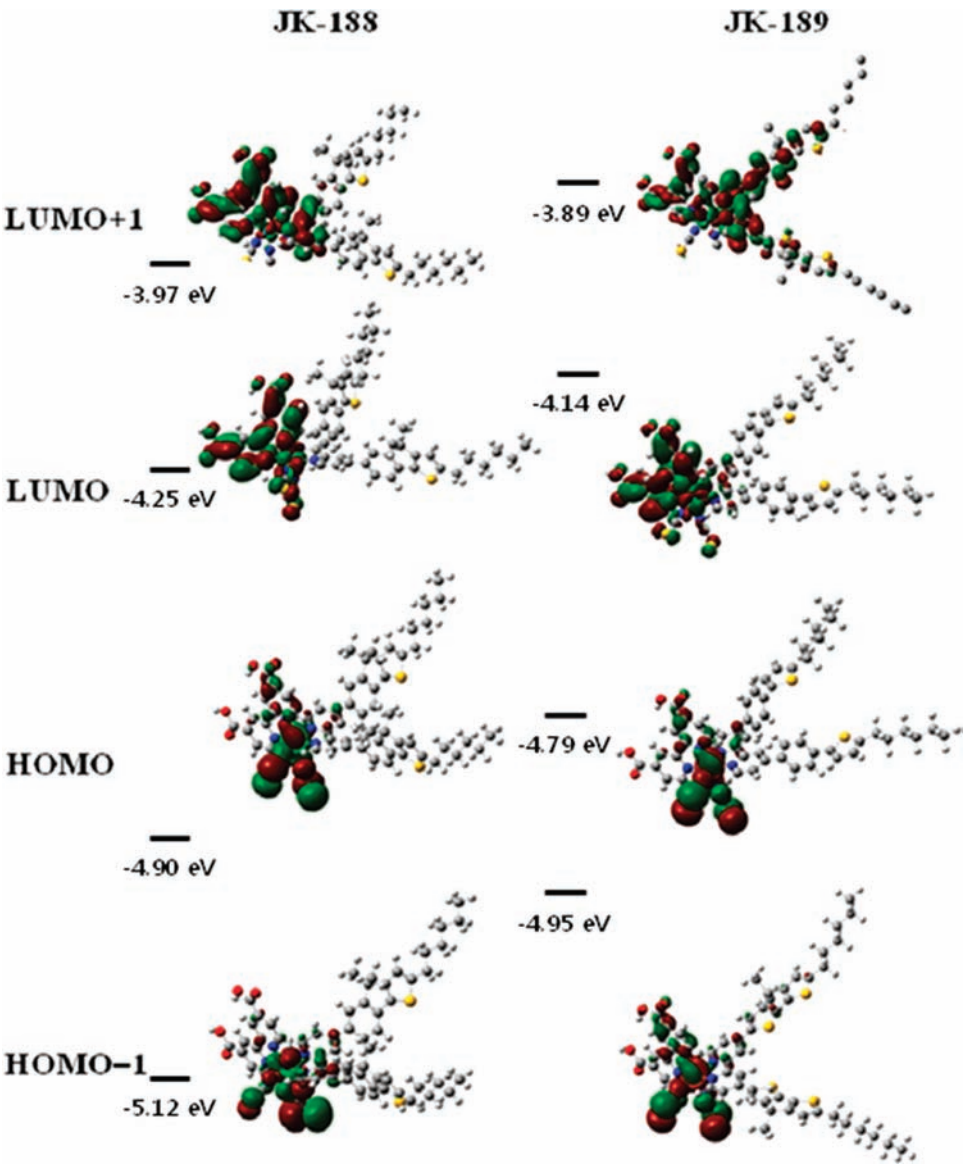

Figure 3. Isodensity surface plots of the HOMO, HOMO−1, LUMO, and LUMO+1 of **JK-188** and **JK-189**.

examination of the HOMO and LUMO of the dyes indicates that HOMO−LUMO excitation moves the electron distribution from the Ru-NCS unit to dcbpy. Accordingly, the change in the electron distribution induced by photoexcitation results in an efficient charge separation.

The photocurrent action spectra of the devices based on **JK-188** and **JK-189** are presented in the inset of Figure 4 and compared with **N719** as a reference. The onsets of photon-to-current conversion efficiency (IPCE) spectra based on **JK-188** and **JK-189** are ca. 810 and 820 nm, respectively. The IPCE spectrum of **JK-189** is red-shifted by about 10−20 nm compared to **JK-188** and **N719** as a result of electron-rich bithiophene π conjugation, which is consistent with the absorption spectrum of **JK-189**. The IPCE spectrum of **JK-189** exceeds 80% in a spectral range from 450 to 610 nm, reaching its maximum of 83% at 538 nm. The $J-V$ curve for the cells based on three sensitizers is presented in Figure 4. The curve integration of **JK-188** over the solar spectrum gives a short-circuit photocurrent density (J_{sc}) of 18.52 mA/cm^2, which is in agreement with the measured photocurrent. The

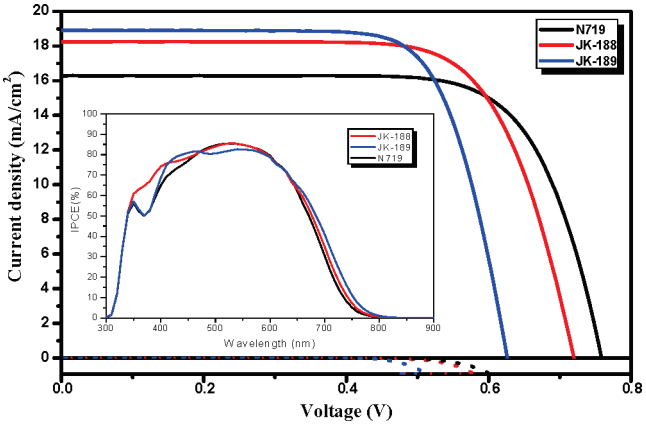

Figure 4. $J-V$ curve and IPCE of **JK-188** (red line), **JK-189** (blue line), and **N719** (black line).

photovoltaic parameters of the cells with an activated cell area of 0.18 cm^2 using a black tape mask are summarized in Table 1. Under standard global AM 1.5 solar conditions, the **JK-188** and **JK-189** sensitized cells gave J_{sc} values of 18.60 and 18.90 mA/cm^2, open-circuit voltages (V_{oc}) of 0.72 and 0.63 V, and fill factors (FFs) of 0.71 and 0.73, yielding overall conversion efficiencies (η) of 9.54 and 8.70%, respectively. Under the same conditions, the **N719** sensitized cell gave a J_{sc} value of 16.28 mA/cm^2, a V_{oc} value of 0.76 V, and an FF of 0.73, yielding η of 9.00%. The efficiency for the **N719** solar cell is about 0.54% inferior to that of the **JK-188** solar cell, although both V_{oc} and FF of the **N719** sensitized cell are close to those of the **JK-188** sensitized cell. The higher η value of the **JK-188** cell compared to that of the **N719** cell comes from the higher J_{sc} value, which can be rationalized by the high absorption coefficient and red-shifted absorption of the MLCT band. On the other hand, the efficiency of **JK-189** is much lower than that of **JK-188** and **N719** in spite of its large photocurrent. Of particular importance is the 90−130 mV increase in V_{oc} of the **JK-188**- and **N719**-based cells relative to the **JK-189**-based cell. This improved V_{oc} value is attributed to suppression of the charge recombination. Minimization of the interfacial charge recombination losses in the devices of both sensitizers is evident from the dark-current data for the cell (Figure 4). To clarify the origin of the charge recombination, we have measured the amounts adsorbed on the TiO_2 film. The adsorbed amounts of 3.18×10^{-7} mmol/cm^2 for **JK-188**, 2.64×10^{-7} mmol/cm^2 for **JK-189**, and 3.47×10^{-7} mmol/cm^2 for **N719** are observed.[14] It seems that the charge recombination is quite sensitive to the molecular structure and the intermolecular $\pi-\pi$ stacking because of the different coverage on the TiO_2 surface, together with the reduction potential.[15]

Because the achievement of long-term stability for DSSCs has became a major issue for a long time, we replaced the liquid electrolyte with a quasi-solid-state one because the device employing the liquid electrolyte has several shortcomings such as leakage and evaporation. Figure 5 shows the photovoltaic performances of **JK-188**- and **JK-189**-based cells during long-term light-soaking and thermal stability

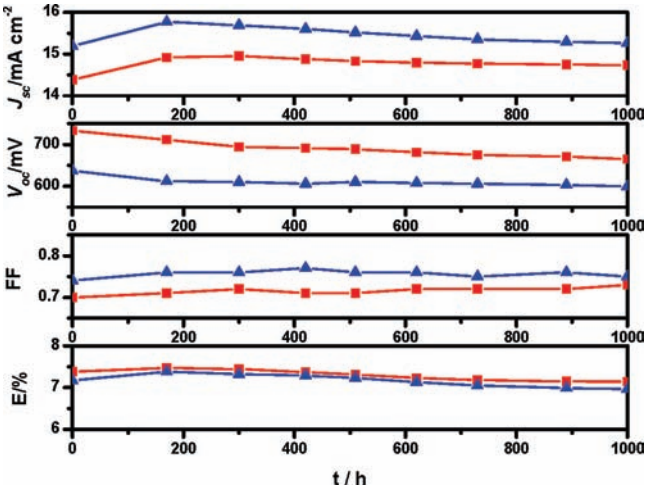

Figure 5. Evolution of the solar-cell parameters with **JK-188** (red ■) and **JK-189** (blue ▲) during visible-light soaking (AM 1.5 G, 100 mW/cm^2) at 60 °C. A 420 nm cutoff filter was placed on the cell surface during illumination. Electrolyte: 5 wt % PVDF-HFP, 0.6 M DMPII, 0.5 M NMBI, and 0.1 M I_2, in MPN.

tests using a polymer gel electrolyte composed of 5 wt % poly(vinylidenefluoride-*co*-hexafluoropropylene) (PVDF-HFP), 0.6 M 1-propyl-2,3-dimethylimidazolium iodide (DMPII), 0.5 M *N*-methylbenzimidazole (NMBI), and 0.1 M I_2 in 3-methoxypropionitrile (MPN). The **JK-188**-based cell yields a strikingly high conversion efficiency of 7.38% (Figure 5). After 1000 h of light soaking at 60 °C, the initial efficiency of 7.38% slightly decreased to 7.14%. After 1000 h of light soaking, V_{oc} decreased by 70 mV, but the loss is compensated for by a gain in J_{sc} from 14.4 to 14.7 mA/cm^2. On the other hand, the efficiency of **JK-189** decreased from 7.17% to 6.96% under the same conditions. Tolerance of such a severe condition by a DSSC having over 7% efficiency is remarkable. Only a few of the ruthenium sensitizers have passed light-soaking and thermal stress tests for 1000 h while retaining an efficiency of over 6% using a quasi-solid-state electrolyte.[16] The long-term stability of **JK-188** and **JK-189** can be attributed to the intrinsic stability of the fused ring and the introduction of long alkyl chains to the fused ring.[17]

Figure 6 shows the electron diffusion coefficients (D_e) and lifetimes (τ_e) of the cells employing **JK-188**, **JK-189**, and **N719** displayed as a function of J_{sc} and V_{oc}, respectively. No significant differences among the D_e values for the three sensitizers were seen at identical short-circuit current conditions, as shown in Figure 6a. The result indicates that the D_e values are hardly affected by structural changes in the dye molecules. On the other hand, the τ_e values show a significant gap among the sensitizers, resulting in the increasing order of **N719** > **JK-188** > **JK-189**. The orders of magnitude of the

(14) Jang, S.-R.; Lee, C.; Choi, H.; Ko, J.; Lee, J.; Vittal, R.; Kim, K.-J. *Chem. Mater.* **2006**, *18*, 5604.
(15) (a) Kim, J.-J.; Choi, H.; Kim, C.; Kang, M.-S.; Kang, H. S.; Ko, J. *Chem. Mater.* **2009**, *21*, 5719. (b) Khazraji, A. C.; Hotchandani, S.; Das, S.; Kamat, P. V. *J. Phys. Chem. B* **1999**, *103*, 4693.
(16) Wang, P.; Zakeeruddin, S. M.; Moser, J. E.; Nazeeruddin, M. K.; Sekiguchi, T.; Grätzel, M. *Nat. Mater.* **2003**, *2*, 402.
(17) (a) Kroeze, J. E.; Hirata, N.; Koops, S.; Nazeeruddin, M. K.; Schmidt-Mende, L.; Grätzel, M.; Durrant, J. R. *J. Am. Chem. Soc.* **2006**, *128*, 16377. (b) Koumura, N.; Wang, Z.-S.; Mori, S.; Miyashita, M.; Suzuki, E.; Hara, K. *J. Am. Chem. Soc.* **2006**, *128*, 14256.
(18) Nakade, S.; Kanzaki, T.; Wada, Y.; Yanagida, S. *Langmuir* **2005**, *21*, 10803.
(19) Kang, M.-S.; Ahn, K.-S.; Lee, J.-W.; Kang, Y. S. *J. Photochem. Photobiol. A: Chem.* **2008**, *195*, 198.
(20) Ahn, K.-S.; Kang, M.-S.; Lee, J.-K.; Shin, B.-C.; Lee, J.-W. *Appl. Phys. Lett.* **2006**, *89*, 013103.
(21) Ahn., K.-S.; Kang, M.-S.; Lee, J.-W.; Kang, Y. S. *J. Appl. Phys.* **2007**, *101*, 084312.

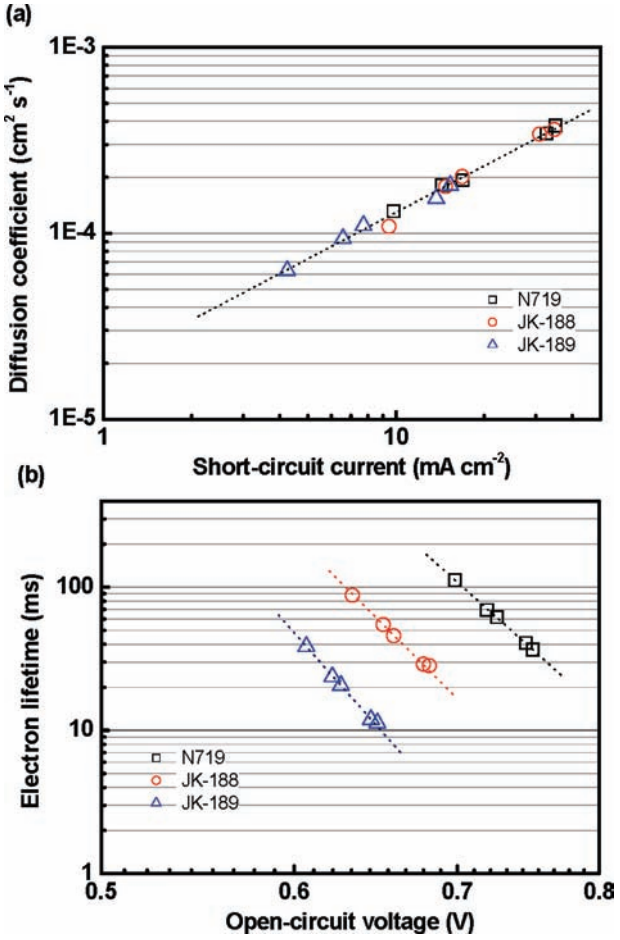

Figure 6. Electron diffusion coefficients (a) and lifetimes (b) in the photoelectrode adsorbing three dyes such as **JK-188**, **JK-189**, and **N719**.

τ_e values (Figure 6b) were largely varied with the structure of the dyes and well consistent with that of V_{oc}, shown in Table 1. The molecular size and structure of **JK-189** reduce dye loading on the TiO_2 surface, giving an increased dark current and lowered V_{oc}. This can be attributable to the electron recombination occurring in the photoelectrodes, where unfilled vacancies were generated by the ineffective packing of larger dyes. The result shows that the structure of **JK-188** is more effective in retarding the electron recombination compared to that of **JK-189** because of the efficient packing of **JK-188**.

To gain more information on the interfacial recombination, electrochemical impedance spectroscopy was performed. Figure 7 shows the alternating-current impedance spectrum measured under dark conditions. In the dark under forward bias (−0.67 V), the semicircle in the intermediate frequency regime demonstrates the dark reaction impedance caused by electron transport from the conduction band of TiO_2 to I_3^- ions in the electrolytes. The increased radius of

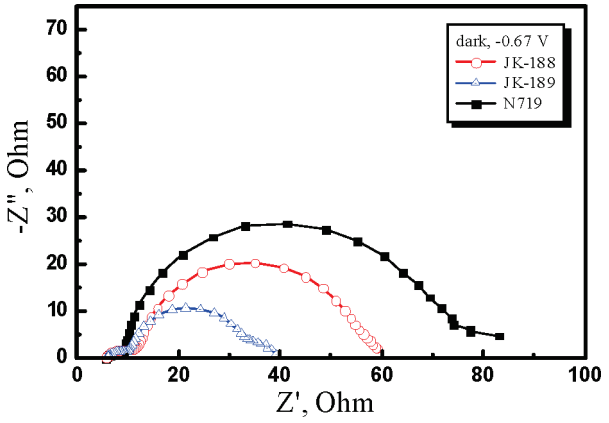

Figure 7. Electrochemical impedance spectra measured in the dark for cells employing different dyes (i.e., **JK-188**, **JK-189**, and **N719**).

the semicircle in the intermediate frequency regime implies a reduced electron recombination rate at the TiO_2/electrolyte interface. From the radius, the increasing order of **N719** (63.81 Ω) > **JK-188** (45.33 Ω) > **JK-189** (29.43 Ω) was obtained, which is in accord with the trends of the V_{oc} and τ_e values.

Conclusion

We have designed and synthesized novel efficient sensitizers **JK-188** and **JK-189** featuring indeno[1,2-*b*]thiophene or a fused dithiophene in the ancillary ligand. A solar-to-electricity conversion efficiency of 9.54% in **JK-188** is better than η of 9.00% for the **N719** sensitized cell, whereas the conversion efficiency of the **JK-188**-based cell using a polymer gel electrolyte gave a strikingly high efficiency of 7.38%. The efficiency is the highest one reported for DSSCs based on the ruthenium sensitizer using a quasi-solid-state electrolyte. Moreover, the **JK-188** device showed excellent stability under a light-soaking test at 60 °C for 1000 h, keeping 97% of the initial performance. The high efficiency and excellent stability of **JK-188** may be attributed to the introduction of an unsymmetrical indeno[1,2-*b*]thiophene unit with a hydrophobic alkyl chain. We believe that the development of highly efficient ruthenium sensitizers with excellent stability is possible through sophisticated structural modifications, and work on these is now in progress.

Acknowledgment. This work was supported by the WCU (the Ministry of Education and Science) program (Grant R31-2008-0001-10035-0) and the Converging Research Center Program through the National Research Foundation of Korea funded by the Ministry of Education, Science and Technology (Grant 2009-0082141)

Supporting Information Available: Syntheses of **JK-188** and **JK-189**. This material is available free of charge via the Internet at http://pubs.acs.org.